# Synthesis, molecular modelling and NLO properties of new ytterbium(iii) complexes with vildagliptin

**J.A. Novoa-López,[1*] P. Martín-Ramos,[2] H. Michinel,[1] I.J. Sola[3] and P. Chamorro-Posada[2]**

[1] *Área de Óptica, Universidade de Vigo, As Lagoas s/n, 32004 Ourense, Spain*
[2] *Dpto. de Teoría de la Señal y Comunicaciones e Ingeniería Telemática, Universidad de Valladolid, ETSI Telecomunicación, Paseo Belén 15, Campus Miguel Delibes, 47011 Valladolid, Spain*
[3] *Universidad de Salamanca, Área de Óptica, Departamento de Física Aplicada, E-37008 Salamanca, Spain*
[*] *joseantonionolo@gmail.com*

**Abstract:** Two nonlinear optical ytterbium(III) complexes with vildagliptin have been synthesized and their ground state geometries have been predicted by semi-empirical quantum chemistry methods: $[Yb(vilda)_3(acac)]$ and $[Yb(vilda)_2(acac)(bipy)]$, where vilda = vildagliptin, acac = acetylacetonate and bipy = 2,2'-bipyridine. ATR-Fourier transform infrared (ATR-FTIR) spectral studies have been carried out to identify the functional groups of the novel complexes. The third order nonlinear optical response has been experimentally studied using Z-scan and P-scan methods, and static and frequency dependent second hyperpolarizabilities have been theoretically investigated using the Sparkle/PM6 model. The novel materials in diluted solutions have nonlinear refractive indices comparable to that of carbon disulphide.



**OCIS codes:** (190.4400) Nonlinear optics, materials; (160.4330) Nonlinear optical materials; (160.5690) Rare-earth-doped materials.

## References and links

1. G. P. Agrawal, *Applications of Nonlinear Fiber Optics,* 2nd ed. (Academic Press, Burlington, 2008).
2. Y. S. Kivshar and G. P. Agrawal, *Optical Solitons: From Fibers to Photonic Crystals* (Academic Press, Burlington, 2003).
3. C. Andraud and O. Maury, "Lanthanide Complexes for Nonlinear Optics: From Fundamental Aspects to Applications," Eur. J. Inorg. Chem. **2009**(29-30), 4357–4371 (2009).
4. J. L. Bredas, C. Adant, P. Tackx, A. Persoons, and B. M. Pierce, "Third-Order Nonlinear Optical Response in Organic Materials: Theoretical and Experimental Aspects," Chem. Rev. **94**(1), 243–278 (1994).
5. N. Sheng, Z. Yuan, J. Wang, W. Chen, J. Sun, and Y. Bian, "Third-order nonlinear optical properties of sandwich-type mixed (phthalocyaninato)(porphyrinato) europium double- and triple-decker complexes," Dyes Pigments **95**(3), 627–631 (2012).
6. L. De Boni, L. Gaffo, L. Misoguti, and C. R. Mendonça, "Nonlinear absorption spectrum of ytterbium bis-phthalocyanine solution measured by white-light continuum Z-scan technique," Chem. Phys. Lett. **419**(4-6), 417–420 (2006).
7. A. B. Karpo, A. V. Zasedatelev, V. E. Pushkarev, V. I. Krasovskii, and L. G. Tomilova, "Influence of blue valence absorption band on nonlinear absorption in dysprosium bisphthalocyanine studied by open aperture z-scan," Chem. Phys. Lett. **585**, 153–156 (2013).
8. A. B. Karpo, V. E. Pushkarev, V. I. Krasovskii, and L. G. Tomilova, "Z-scan study of nonlinear absorption in novel lanthanide bis-phthalocyanines," Chem. Phys. Lett. **554**, 155–158 (2012).
9. H. Hou, Y. Wei, Y. Song, Y. Fan, and Y. Zhu, "First Octameric Ellipsoid Lanthanide(III) Complexes: Crystal Structure and Nonlinear Optical Absorptive and Refractive Properties," Inorg. Chem. **43**(4), 1323–1327 (2004).
10. W. P. Gillin and R. J. Curry, "Erbium (III) tris(8-hydroxyquinoline) (ErQ): A potential material for silicon compatible 1.5 μm emitters," Appl. Phys. Lett. **74**(6), 798 (1999).
11. F. Wei, Y. Z. Li, G. Z. Ran, and G. G. Qin, "1.54 μm electroluminescence from p-Si anode organic light emitting diode with Bphen: $Er(DBM)_3$phen as emitter and Bphen as electron transport material," Opt. Express **18**(13), 13542–13546 (2010).
12. J. Leuthold, W. Freude, J.-M. Brosi, R. Baets, P. Dumon, I. Biaggio, M. L. Scimeca, F. Diederich, B. Frank, and C. Koos, "Silicon Organic Hybrid Technology - A Platform for Practical Nonlinear Optics," Proc. IEEE **97**(7), 1304–1316 (2009).

#228473 - $15.00 USD Received 25 Nov 2014; revised 15 Jan 2015; accepted 17 Jan 2015; published 6 Feb 2015

13. F. J. Fraile-Peláez, P. Chamorro-Posada, and R. Gómez-Alcalá, "Racetrack Add-Drop Resonator with an Organic Cover for Nonlinear Switching Enhancement," J. Nonlinear Opt. Phys. Mater. **21**(03), 1250030 (2012).
14. J. J. P. Stewart, MOPAC2012, Stewart Computational Chemistry, Colorado Springs, CO, USA, 2012.
15. D. Briers, I. Picard, T. Verbiest, A. Persoons, and C. Samyn, "Nonlinear optical active poly(adamantyl methacrylate-methyl vinyl urethane)s functionalised with phenyltetraene-bridged chromophore," Polymer (Guildf.) **45**(1), 19–24 (2004).
16. S. Janarthanan, R. Sugaraj Samuel, Y. C. Rajan, P. Suresh, and K. Thangaraj, "Growth of N-Glycyl-l-Valine (GV) single crystal and its spectral, thermal and optical characterization," Spectrochim. Acta, Pt. A: Mol. Biomol. Spectrosc. **105**, 34–37 (2013).
17. C. Lin, K. Wu, M. Zhang, and C. Mang, "Theoretical studies on hyperpolarizabilities and UV-Vis-IR spectra of a diamminecobalt(III) tetripeptide transition-metal complex," PhysChemComm **6**(15), 59 (2003).
18. R. O. Freire and A. M. Simas, "Sparkle/PM6 Parameters for all Lanthanide Trications from La(III) to Lu(III)," J. Chem. Theory Comput. **6**(7), 2019–2023 (2010).
19. J. J. P. Stewart, "Optimization of parameters for semiempirical methods V: Modification of NDDO approximations and application to 70 elements," J. Mol. Model. **13**(12), 1173–1213 (2007).
20. A.-R. Allouche, "Gabedit--A graphical user interface for computational chemistry softwares," J. Comput. Chem. **32**(1), 174–182 (2011).
21. R. O. Freire, N. B. da Costa, G. B. Rocha, and A. M. Simas, "Sparkle/PM3 Parameters for the Modeling of Neodymium(III), Promethium(III), and Samarium(III) Complexes," J. Chem. Theory Comput. **3**(4), 1588–1596 (2007).
22. Z. A. Fekete, E. A. Hoffmann, T. Körtvélyesi, and B. Penke, "Harmonic vibrational frequency scaling factors for the new NDDO Hamiltonians: RM1 and PM6," Mol. Phys. **105**(19-22), 2597–2605 (2007).
23. S. P. Karna and M. Dupuis, "Frequency dependent nonlinear optical properties of molecules: Formulation and implementation in the HONDO program," J. Comput. Chem. **12**(4), 487–504 (1991).
24. R. A. Ganeev, A. I. Ryasnyansky, M. Baba, M. Suzuki, N. Ishizawa, M. Turu, S. Sakakibara, and H. Kuroda, "Nonlinear refraction in $CS_2$," Appl. Phys. B **78**(3-4), 433–438 (2004).
25. U. Tripathy and P. B. Bisht, "Influence of pulsed and cw pumping on optical nonlinear parameters of laser dyes probed by a closed-aperture Z-scan technique," J. Opt. Soc. Am. B **24**(9), 2147–2156 (2007).
26. A. G. Orpen, L. Brammer, F. H. Allen, O. Kennard, D. G. Watson, and R. Taylor, "Supplement. Tables of bond lengths determined by X-ray and neutron diffraction. Part 2. Organometallic compounds and co-ordination complexes of the d- and f-block metals," Dalton Trans. (12): S1 (1989).
27. C. K. Pearce, D. W. Grosse, and W. Hessel, "Effect of molecular structure on infrared spectra of six isomers of bipyridine," J. Chem. Eng. Data **15**(4), 567–570 (1970).
28. G. Deacon, "Relationships between the carbon-oxygen stretching frequencies of carboxylato complexes and the type of carboxylate coordination," Coord. Chem. Rev. **33**(3), 227–250 (1980).
29. L.-J. Bian, H.-A. Xi, X.-F. Qian, J. Yin, Z.-K. Zhu, and Q.-H. Lu, "Synthesis and luminescence property of rare earth complex nanoparticles dispersed within pores of modified mesoporous silica," Mater. Res. Bull. **37**(14), 2293–2301 (2002).
30. S. Nunn and K. Nishikida, "Advanced ATR Correction Algorithm - Application Note 50581," (Madison, WI, USA., 2008).
31. R. W. Boyd, *Nonlinear Optics,* 3rd ed. (Academic Press, 2008).
32. M. Sheik-Bahae, A. A. Said, T. H. Wei, D. J. Hagan, and E. W. Van Stryland, "Sensitive measurement of optical nonlinearities using a single beam," IEEE J. Quantum Electron. **26**(4), 760–769 (1990).
33. M. Falconieri, "Thermo-optical effects in Z -scan measurements using high-repetition-rate lasers," J. Opt. **1**, 662–667 (1999).
34. R. L. Sutherland, *Handbook of Nonlinear Optics,* 2nd ed. (CRC Press, 2003).
35. J. L. Oudar and D. S. Chemla, "Hyperpolarizabilities of the nitroanilines and their relations to the excited state dipole moment," J. Chem. Phys. **66**(6), 2664–2668 (1977).
36. J. L. Oudar, "Optical nonlinearities of conjugated molecules. Stilbene derivatives and highly polar aromatic compounds," J. Chem. Phys. **67**(2), 446–457 (1977).
37. A. Gulino, I. L. Fragalà, F. Lupo, G. Malandrino, A. Motta, A. Colombo, C. Dragonetti, S. Righetto, D. Roberto, R. Ugo, F. Demartin, I. Ledoux-Rak, and A. Singh, "Fascinating Role of the Number of f Electrons in Dipolar and Octupolar Contributions to Quadratic Hyperpolarizability of Trinuclear Lanthanides-Biscopper Schiff Base Complexes," Inorg. Chem. **52**(13), 7550–7556 (2013).
38. H. S. Nalwa and S. Miyata, *Nonlinear Optics of Organic Molecules and Polymers* (Taylor & Francis, 1996).

## 1. Introduction

The development of high-performance all-optical photonic processing devices based on self- or cross-phase modulation effects [1] or optical solitons [2] relies on the buildup of new highly transparent optical materials with a large and fast third-order nonlinear response. The use of lanthanide complexes as nonlinear optical media is a highly promising and largely unexplored field [3]. In particular, very few studies on the third-order nonlinear properties of lanthanide complexes exist. Multi-decker phtalocyanine and prophirine lanthanide complexes have attracted attention due to their very large and fast third order susceptibility [4,5] and their non-linear absorption properties [6–8]. A very intriguing behavior has been observed in

#228473 - $15.00 USD Received 25 Nov 2014; revised 15 Jan 2015; accepted 17 Jan 2015; published 6 Feb 2015

the case of two La and Ce isostructural octameric complexes [9]: one of them showed no nonlinear absorption and a strong nonlinear refraction while the other presented the complementary behavior in its third order nonlinear optical properties. This type of lanthanide complexes have also been demonstrated to be compatible with Si technology [10,11] and could also be employed for nonlinear hybrid-silicon photonics applications [12,13] in the second and third optical communication windows.

We present an experimental and theoretical study of two new ytterbium(III) complexes with vildagliptin that are shown to exhibit large nonlinear refraction and very low nonlinear absorption in methanol diluted solutions. The third order nonlinear properties of the new materials have been experimentally measured at the first telecom window (810 nm) and their nonlinear optical properties have been investigated using computational quantum chemistry methods. The geometry of the new complexes, the vibrational frequencies and their static and frequency dependent (evaluated at the three telecom windows) second hyperpolarizabilities have been computed using the Sparkle/PM6 model implemented in MOPAC2012 [14].

Vildagliptin (previously identified as LAF237, trade names Zomelis, Galvus) is an oral anti-hyperglycemic agent (anti-diabetic drug) of the new dipeptidyl peptidase-4 (DPP-4) inhibitor class of drugs. Its chemical systematic name is (S)-1-[N-(3-hydroxy-1-adamantyl)glycyl]pyrrolidine-2-carbonitrile and its structure is shown in Fig. 1.

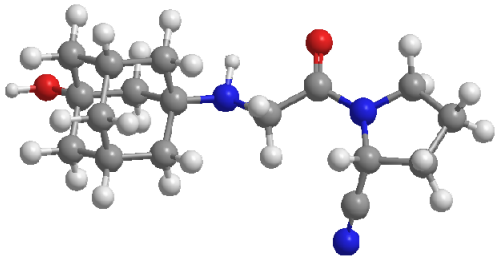

Fig. 1. Vildagliptin structure.

In the molecule, the hydroxyl-adamantyl and pyrrolidine-2-carbonitrile moieties, linked by glycyl (gly, the amino acid radical or residue –$HNCH_2CO$– of glycine), can be identified.

Some adamantyl and glycyl derivatives have been reported to have NLO response in the past, such as poled films of poly(adamantyl methacrylate-methylvinylurethane) [15], single crystals of N-glycyl-l-valine [16] and transition-metal complexes as $Co(NH_3)_2$(L-ala–gly–gly) [17]. Nevertheless, these previous works have focused on the second order NLO properties of those materials. We hereby address the third order nonlinear response of vildagliptin, with a constructive association of adamantyl and glycyl entities and the additional presence of the pyrrolidine-2-carbonitrile substituent. Moreover, the impact of the incorporation of vildagliptin into lanthanide complexes as a ligand for the achievement of high nonlinear refractive index chromophores is also investigated. Thus, we have synthesized two ytterbium(III) complexes with vildagliptin, [Yb(vilda)$_3$(acac)] and [Yb(vilda)$_2$(acac)(bipy)] (where vilda = vildagliptin, acac = acetylacetonate and bipy = 2,2'-bipyridine) and studied their NLO properties with a view to their presumable applications in Optoelectronics.

## 2. Experimental

### *2.1 Synthesis*

All reagents and solvents employed, except for vildagliptin, were commercially available and used as supplied without further purification: acetylacetone (CAS No. 123-54-6, Sigma-Aldrich, >99%); 2,2'-bipyridine (CAS No. 366-18-7, Sigma-Aldrich, >99%); $Yb(NO_3)\cdot 5H_2O$ (CAS No. 35725-34-9, Sigma-Aldrich, 99.999%); $CH_3OK$ (CAS No. 865-33-8, Sigma-Aldrich, 95%); $CH_3OH$ (CAS No. 67-56-1, Sigma-Aldrich, 99.8%); and 1,4-dioxane (CAS No. 123-91-1, Sigma-Aldrich, 99.8%). Vildagliptin was supplied by Novartis (Galvus®) and purified (recrystallized) in methanol.

#228473 - $15.00 USD Received 25 Nov 2014; revised 15 Jan 2015; accepted 17 Jan 2015; published 6 Feb 2015

Tris((S)-1-[N-(3-hydroxy-1-adamantyl)glycylate]pyrrolidine-2-carbonitrile)mono(2,2'-bipyridine)ytterbium(III), named [Yb(vilda)$_3$(bipy)] (Table 1), was obtained as follows: under stirring, a purified vildagliptin (3 mmol) methanol solution (20 mL) was added to a 1 mmol of $Yb(NO_3)_3 \cdot 5H_2O$ in methanol. The mixture was neutralized by adding potassium methoxide (3 mmol) dropwise under vigorous stirring until potassium nitrate precipitated. $KNO_3$ was removed by decanting, and bipy (1 mmol) was finally added. The mixture was heated to 75°C and stirred overnight, then washed with dioxane, and finally dried in vacuum to give product in 90-95% yield (based on Yb). The synthetic procedure for bis((S)-1-[N-(3-hydroxy-1-adamantylate)glycylate]pyrrolidine-2-carbonitrile)mono(acetylacetonate)mono(2,2'-bipyridine)ytterbium(III), i.e. [Yb(vilda)$_2$(acac)(bipy)] (Table 1), was entirely analogous, except for the initial methanol solution, which in this case consisted of 2 mmol of vildagliptin and 1 mmol of acetylacetone (Hacac). All the procedures for complex preparation were carried out under nitrogen and using dry reagents to avoid the presence of water and oxygen, which can quench metal photoluminescence.

**Table 1. Elemental analysis data for the two complexes**

| Complex | | [Yb(vilda)$_3$(bipy)] | [Yb(vilda)$_2$(acac)(bipy)] |
|---|---|---|---|
| Chemical formula | | $C_{61}H_{80}N_{11}O_6Yb$ | $C_{49}H_{64}N_8O_6Yb$ |
| $M_W$ (g/mol) | | 1236.44 | 1034.16 |
| Anal. Calcd. (%) | C | 59.26 | 56.91 |
| | H | 6.52 | 6.24 |
| | N | 12.46 | 10.84 |
| | O | 7.76 | 9.28 |
| | Yb | 14.00 | 16.73 |
| Found | C | 59.86 | 57.03 |
| | H | 6.71 | 6.30 |
| | N | 12.16 | 11.02 |

### *2.2. Computational procedure*

The estimation of the unknown geometries was based on calculations using the Sparkle/PM6 model [18,19] implemented in the MOPAC2012 package [14]. The Sparkle model permits to include the lanthanide series in semi-empirical quantum chemistry calculations by replacing the lanthanide ion with a charge of + 3e superimposed to a repulsive exponential potential that mimics the effect of the size of the ion. Additionally, two Gaussian functions permit to model the core-core repulsion energy term and the inclusion of the lanthanide mass allows the calculation of vibrations and thermochemical quantities. The Sparkle/PM6 model is designed to reproduce the coordinating polyhedral of the complexes and high quality crystallographic structures from the Cambridge Structural Database (CSD), and *ab-initio* calculations have been used for the derivation of the model parameters [18].

For each complex, several initial seed configurations with varying arrangements of the ligands were prepared with the aim of exploring as many of all the relative orientations of the ligands as possible. Each of these configurations was pre-optimized using the Molecular Mechanics implementation in Gabedit [20] and fully optimized using the Sparkle/PM6 model in MOPAC2012. From each of the resulting configurations, 200 different input geometries were generated by applying a random rotation and a random translation to each of the ligands, as described in [21]. A PM6/Sparkle optimization was then performed for each of these random geometries. Typically, among the 200 outputs obtained from one seed configuration, a series of faulty results (e.g. geometries with uncoordinated ligands) are found, together with a number of clusters of essentially identical output geometries. As it is proposed in [21], we have chosen the resulting properly optimized configuration with the lowest total energy as our estimate for the unknown complex geometry.

The vibrational frequencies for the estimated geometries were computed using the PM6/Sparkle model implemented in MOPAC2012 and corrected using the scale factors given in [22]. The corresponding estimated IR spectra were represented using Gabedit. The

#228473 - $15.00 USD Received 25 Nov 2014; revised 15 Jan 2015; accepted 17 Jan 2015; published 6 Feb 2015

(microscopic) static and dynamic molecular second hyperpolarizabilities [23] have also been calculated with MOPAC2012 using the Sparkle/PM6 model.

### *2.3. Physical measurements*

The C, H, N elemental analyses for the two complexes were conducted using a Perkin Elmer CHN 2400 apparatus.

The infrared spectra were recorded with a Thermo Nicolet 380 FT-IR apparatus equipped with Smart Orbit Diamond ATR system.

### *2.4. NLO characterization procedure*

The experimental setup, depicted in Fig. 2, included a titanium-sapphire laser source (Tsunami, Spectra Physics) operating at a wavelength of 810 nm. The temporal duration of the pulses was 80 fs and the repetition rate was 80.75 MHz. The maximum average power of this laser was 2 W. The system was calibrated using carbon disulfide ($CS_2$), a very well characterized material known to be a good reference. Our $CS_2$ measurements have been in agreement with those published by other groups, such as Ganeev *et al*. [24].

The first part of the system consisted of two lenses, labeled $L_1$ and $L_2$. These lenses were used to collimate and select the beam size incident on $L_3$ with focal length $f$ = 15 cm, which focused the laser on the sample (*S*). The half-waveplate ($W_1$) and the polarizing-cube ($PC_1$) were used to change the incident power at the sample. The beam waist in the focal plane of $L_3$ had a value of 19 μm (measured at $1/e^2$) with a $z_0$ = 1.4 mm. The sample was placed on a moving track that enabled the displacement of the sample along the *z*-axis around the focal point.

$L_4$ was a lens with a focal length $f$ = 25 cm and it was used to collimate the beam to a size that allowed the use of the detectors. With the second pair of polarizing-cube ($PC_2$) and half-waveplate ($W_2$), the beam leaving the sample was split between the two detectors which were at the end of each path. The first signal came from a fast photodiode (*PH*) with a response time of nanoseconds, located behind a diaphragm ($AP_1$), which was used to obtain the experimental curve for the calculation of the nonlinear refractive index. A neutral filter (*NF*) was positioned before *PH* to avoid damage by the beam. The second measurement was performed with a powermeter (*PW*), placed in front of a lens ($L_5$) that focused the beam in order to measure the nonlinear absorbance. The $AP_2$ diaphragm was used to measure the nonlinear refractive index with *PW* when required.

To obtain the Z-scan measurements of transmittance, the position of the sample was scanned from –20 mm to 20 mm. The transmittance curve of the closed aperture Z-scan was detected with *PH* and the transmittance curve of the open aperture Z-scan was detected with *PW*. To use this system for a P-scan, the sample was placed at the maximum of transmittance (previously determined in the Z-scan) and then a power scan was performed.

For the preparation of the samples solutions, the complexes were dissolved in methanol. The corresponding solution was then placed inside a quartz cuvette (which transmitted 88% of incident light) with 1 mm thickness. This thickness was large enough so that the media would not recover the initial conditions between each laser pulse, and thus the materials displayed cumulative thermal effects leading to a negative thermo-optical response.

So as to characterize the Kerr response of the materials, the same system with a laser source with a different repetition rate was used, as in the work by Tripathy *et al.* [25]. This laser source also operated at a wavelength of 810 nm. The temporal duration of the pulses was 20 fs and the repetition rate was 1 kHz. The maximum average power of this laser was also 2 W, with a maximum energy per pulse of 2.11 mJ. With this source, the waist in the focal plane of $L_3$ had a value of 25.4 μm (measured at $1/e^2$) with a $z_0$ = 2.5 mm.

#228473 - $15.00 USD Received 25 Nov 2014; revised 15 Jan 2015; accepted 17 Jan 2015; published 6 Feb 2015

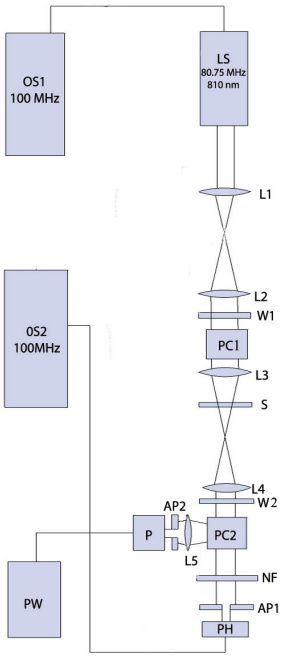


Fig. 2. Sketch of the experimental setup, where *LS* is the laser source, *PH* is the photodiode, *PW* is the powermeter, *AP* is diaphragm, *W* is waveplate, *L* is lens, *PC* is polarizing-cube, *NF* is neutral filter, *S* represents the sample and *OS* stands for oscilloscope.

## 3. Results and discussion

### *3.1. Predicted molecular conformations*

The ground state geometries of the two novel complexes were predicted using the Sparkle/PM6 model and are shown in Fig. 3 and Fig. 4. Yb-N distances and Yb-O distances are provided in Table 2, and are within normal ranges [26].

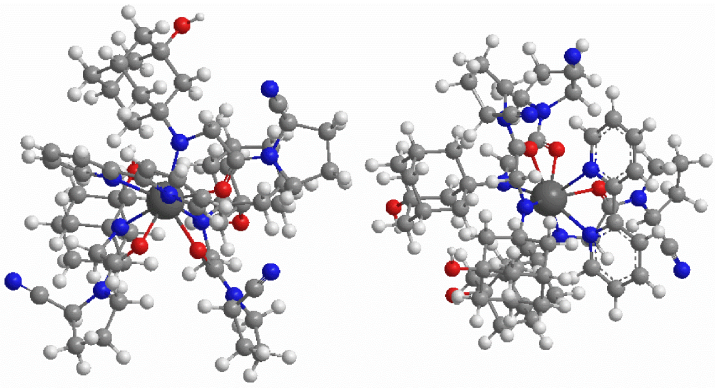

Fig. 3. Two views of the predicted ground state geometry for [Yb(vilda)$_3$(bipy)].

#228473 - $15.00 USD Received 25 Nov 2014; revised 15 Jan 2015; accepted 17 Jan 2015; published 6 Feb 2015

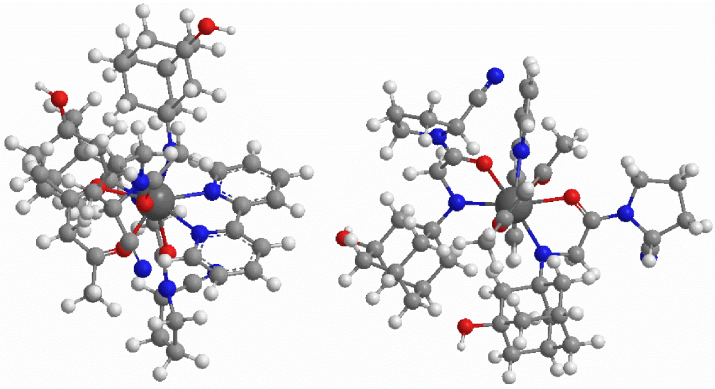

Fig. 4. Two views of the predicted ground state geometry for [Yb(vilda)$_2$(acac)(bipy)].

**Table 2. Yb-N and Yb-O distances in Å.**

| Bond | [Yb(vilda)$_3$(bipy)] | Bond | [Yb(vilda)$_2$(acac)(bipy)] |
|---|---|---|---|
| Yb-N1 | 2.424 | Yb-N1 | 2.408 |
| Yb-N2 | 2.410 | Yb-N2 | 2.402 |
| Yb-O1 | 2.391 | Yb-O1 | 2.376 |
| Yb-N3 | 2.308 | Yb-N3 | 2.304 |
| Yb-O2 | 2.390 | Yb-O2 | 2.377 |
| Yb-N4 | 2.306 | Yb-N4 | 2.299 |
| Yb-O3 | 2.393 | Yb-O3 | 2.325 |
| Yb-N5 | 2.305 | Yb-O4 | 2.334 |

*3.2. Infrared spectroscopy*

The wealth of functional groups in vildagliptin (mainly, hydroxy-1-adamantyl and pyrrolidine) and their high representation in the complex determined that most of the bands of the spectra can be assigned to this ligand. However, there is also evidence of coordination of the 2,2'-bipyridine ancillary ligand and, in the case of [Yb(vilda)$_2$(acac)(bipy)] complex, of the formation of $Yb^{3+}$-acetylacetonate coordination bonds.

Thus, the bands observed between 1465 and 1450 $cm^{-1}$ and 1060-1045 $cm^{-1}$ are assigned, respectively, to CN and CC ring stretching modes from 2,2'-bipyridine [27]. They are shifted in comparison with those of the free ligand, suggesting that 2,2'-bipyridine is in fact coordinated to ytterbium(III) [27,28]. An analysis of the region below 1100 $cm^{-1}$ also allows us to see the characteristic absorption bands of coordinated 2,2'-bipyridine at 762 $cm^{-1}$ (C-H out of plane bending mode) and at 657 $cm^{-1}$ (ring deformation mode). The bands that appear between 584 and 535 $cm^{-1}$, which should assigned to a ν(Yb-N) vibration, offer additional evidence of the fact that the coordination bonds have been formed between $Yb^{3+}$ and bipy [29].

Other bands of interest in the fingerprint region are: 1653 $cm^{-1}$ (either a vildagliptin C = O (enol form) stretching mode or a C = N stretching mode); 1620 $cm^{-1}$ (acetylacetonate C = O (enol form) stretching mode); 1407-1404 $cm^{-1}$ ($CH_3$ asymmetric deformation mode); 1353-1348 $cm^{-1}$ (C = O stretching mode); 1258-1256 $cm^{-1}$ (C-O stretching mode); 1148 $cm^{-1}$ (CH in plane bending mode; 1012-970 $cm^{-1}$ (C-H rocking mode); and 915-913 $cm^{-1}$ (C-$CH_3$ stretching mode).

In the 3500-2100 $cm^{-1}$ region, bands between 2975 and 2800 $cm^{-1}$ are assigned to C-H stretching of adamantyl and that at 2238 $cm^{-1}$ to nitrile CN stretching. Finally, the small absorption in the 3500-3000 $cm^{-1}$ region, attributed to OH stretching vibrations, is the expected for a low amount of OH groups, as planned in the preparative conditions.

#228473 - $15.00 USD Received 25 Nov 2014; revised 15 Jan 2015; accepted 17 Jan 2015; published 6 Feb 2015

Comparison of simulated FTIR spectra vs. experimental ATR-FTIR spectra

The simulated infrared spectra, depicted in Fig. 5, exhibit a morphology similar to those obtained experimentally by ATR-FTIR, supporting the good accuracy of the semi-empirical quantum chemical methods used to predict the ground state geometries of the two complexes. The calculated frequencies and intensities are shown in the figure as vertical lines. The estimate of the absorption spectrum has been obtained by assuming a Lorentzian line shape with a spectral half-width set arbitrarily to 20 nm for each resonance. Some of the differences between the two may be in fact related to the ATR technique, which introduces distortion of the relative intensities of bands and absolute shifts in frequency [30].

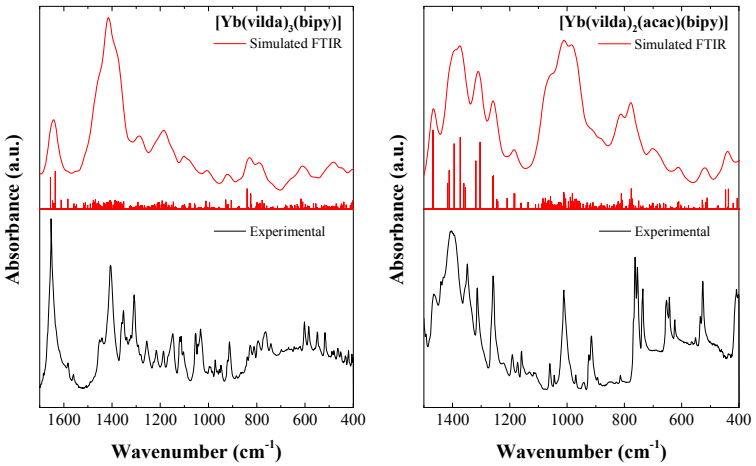


Fig. 5. Comparison of simulated *vs*. experimental FTIR for [Yb(vilda)$_3$(bipy)] (*left*) and [Yb(vilda)$_2$(acac)(bipy)] (*right*) in the fingerprint region.

### *3.3. NLO characterization*

As noted above, the NLO measurements for vildagliptin, [Yb(vilda)$_3$(bipy)] and [Yb(vilda)$_2$(acac)(bipy)] samples were conducted in methanol diluted solutions ($5 \times 10^{-3}$ M). The nonlinear refractive index of methanol is one order of magnitude lower than those of vildagliptin and the two complexes and it is also much lower than that of $CS_2$ [31]. Measurements with pure methanol (99.9%) were carried out in the same conditions so as to evaluate its impact on the measurements accuracy, but no changes in the transmittance curves were detected. $CS_2$ measurements were also conducted so as to have a suitable reference to compare the nonlinear refractive indices of the novel materials to (see Table 3).

For a high repetition rate, the transmittance curves -Fig. 6, in red color- obtained by Z-scan technique for vildagliptin, [Yb(vilda)$_3$(bipy)] and [Yb(vilda)$_2$(acac)(bipy)] show a negative thermo-optical response and were obtained in accordance with the Z-scan theory described by Sheik-Bahae *et al*. [32], where $n_2^{Thermal}$ is the value calculated from the experimental data considering an equivalent Kerr medium. $\theta$ is the thermal induced phase shift [33], and the value of $\theta$ was determined by using the thermal lens formalism described by M. Falconieri [33]. The average ratio $\theta/P_{Thermal}$ allows making a comparison between the strength of the nonlinear refraction observed in the complexes [33]. The experimental values obtained from P-scan are in agreement with those obtained from Z-scan. The results of these measurements are summarized in Table 3.

As it has been indicated above, it is possible to obtain either Kerr or thermo-optical response by working with different repetition rates [25]. Figure 6 (*black*) shows that, for the laser source at 1 kHz, the samples of vildagliptin and the two complexes display a positive Kerr behavior, since in this case thermal effects are not accumulated. The obtained values for

#228473 - $15.00 USD Received 25 Nov 2014; revised 15 Jan 2015; accepted 17 Jan 2015; published 6 Feb 2015

Z-scan and P-scan of the Kerr nonlinear refractive index ($n_2^{Kerr}$) in this case are summarized in Table 3 too.

The errors in $n_2^{Kerr/Thermal}$ and $\beta$ were determined by calculating the standard deviation of several measurements made in $CS_2$. The linear refractive indexes ($n_0$) shown in Table 3 were measured by using a sodium spectrometer (589.6 nm).

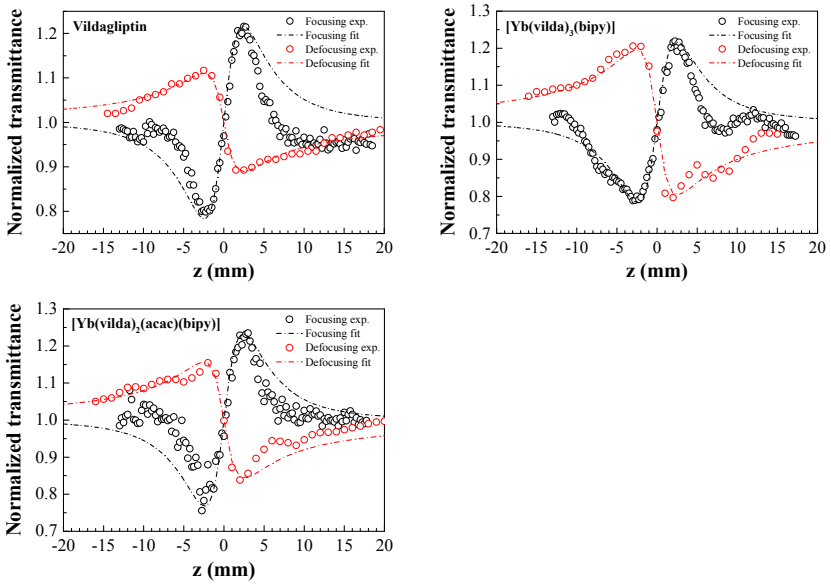


Fig. 6. Z-scan closed-aperture measurements for vildagliptin, [Yb(vilda)$_3$(bipy)] and [Yb(vilda)$_2$(acac)(bipy)] samples when excited with a 80.75 MHz laser source (*red circles*) and with a 1 kHz laser source (*black circles*), and their respective numerical calculations in the Thermal lens formalism (*red dashed line*) and Sheik-Bahae formalism (*black dashed line*).

**Table 3. Optical characterization of vildagliptin complexes in methanol, where $\theta$ is the thermal induced phase shift, $\beta$ is the nonlinear absorption coefficient, $\Delta T_{pv}^{Kerr/Thermal}$ is the peak-valley difference and $P_{Kerr/Thermal}$ is the average power used.**

| | Vildagliptin | [Yb(vilda)$_3$(bipy)] | [Yb(vilda)$_2$(acac)(bipy)] | $CS_2$ |
|---|---|---|---|---|
| $n_0$ | 1.389 | 1.449 | 1.464 | 1.63 [31] |
| $n_2^{Kerr}$ ($m^2$/W) | $6.6 \pm 0.5 \times 10^{-19}$ | $6.4 \pm 0.5 \times 10^{-19}$ | $7.3 \pm 0.5 \times 10^{-19}$ | $1.2 \pm 1 \times 10^{-18}$ |
| $\chi^{(3)Kerr}$ ($m^2/V^2$) | $4.5 \times 10^{-21}$ | $4.8 \times 10^{-21}$ | $5.5 \times 10^{-21}$ | $1.1 \times 10^{-20}$ |
| $\gamma^{Kerr}$ ($m^5/V^2$) | $6.0 \times 10^{-46}$ | $6.3 \times 10^{-46}$ | $7.4 \times 10^{-46}$ | $4.5 \times 10^{-49}$ |
| $n_2^{Thermal}$ ($m^2$/W) | $-0.9 \pm 0.5 \times 10^{-18}$ | $-1 \pm 0.5 \times 10^{-18}$ | $-0.7 \pm 0.5 \times 10^{-18}$ | $-1 \pm 0.2 \times 10^{-18}$ |
| Concentration | $5 \times 10^{-3}$ M | $5 \times 10^{-3}$ M | $5 \times 10^{-3}$ M | Non-diluted (99.9% pure) |
| $\beta$ (m/W) | Not present | Not present | $6 \pm 0.3 \times 10^{-14}$ | $6.1 \pm 0.5 \times 10^{-13}$ |
| $\Delta T_{pv}^{Kerr}$ | 0.43 | 0.42 | 0.48 | – |
| $\Delta T_{pv}^{Thermal}$ | 0.22 | 0.41 | 0.25 | – |
| $\theta$ | 0.21 | 0.38 | 0.26 | – |
| $P_{Kerr}$ (W) | $5.9 \times 10^{-6}$ | $5.9 \times 10^{-6}$ | $5.9 \times 10^{-6}$ | – |
| $P_{Thermal}$ (W) | 0.105 | 0.176 | 0.144 | – |
| $\theta/P_{Thermal}$ | 2 | 2.2 | 1.8 | – |

Several considerations should be raised in view of Table 3. The $n_2^{Thermal}$ of vildagliptin and the complexes are comparable to the value obtained for $CS_2$. The increase of $\theta/P_{Thermal}$ ratio with the size of the vildagliptin complexes makes possible to design complexes with higher nonlinearities of thermal origin. Furthermore, it is noteworthy that vildagliptin and [Yb(vilda)$_3$(bipy)] show negligible nonlinear absorption, while this feature is not present when one of the vildagliptin units is substituted by other ligands, such as acac, as depicted in

#228473 - $15.00 USD Received 25 Nov 2014; revised 15 Jan 2015; accepted 17 Jan 2015; published 6 Feb 2015

Fig. 7. The presence of two photon nonlinear absorption in [Yb(vilda)$_2$(acac)(bipy)] suggests optical limiting as a potential application. The numerical calculation of the two photon nonlinear absorption, represented in Fig. 7 as a dashed line, has been carried out according to Sheik-Bahae *et al*. [32]. The asymmetry in the experimental data can be due to the finite size of the detector, which may clip a small portion of the beam, and/or to the fact that nonlinear refraction may distort the signal.

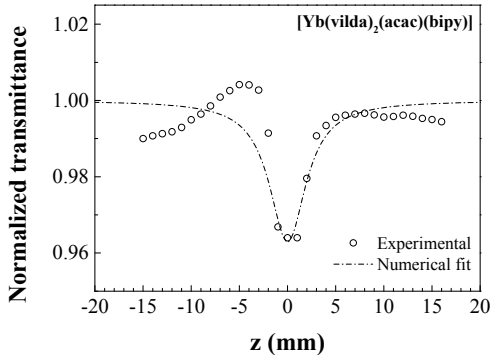


Fig. 7. Z-scan open-aperture measurement of the absorbance for [Yb(vilda)$_2$(acac)(bipy)] sample ($L$ = 1 mm) with P = 1.734 W and 80.75 MHz repetition rate: experimental values (*open circles*) *vs*. numerical calculation (*dashed line*).

The $n_2^{Kerr}$ for the materials under study is lower than that of $CS_2$. Nonetheless, it is worth pointing out that, although vildagliptin and its complexes were assessed in methanol diluted solutions, their $n_2^{Kerr}$ values are only a factor of 2 smaller than that of non-diluted $CS_2$. The values of the third order susceptibility, $\chi^{(3)Kerr}$, and the second-order hyperpolarizability, $\gamma$, have been calculated from the $n_2^{Kerr}$ measurements according to the literature [5,31,34]. The values obtained for $\chi^{(3)Kerr}$ show the same behavior as the $n_2^{Kerr}$, and are only a factor of 2 smaller than that of non-diluted $CS_2$, whereas the values of $\gamma^{Kerr}$ in these compounds are three orders of magnitude higher than that of non-diluted $CS_2$ (see Table 3). It can be expected that, if the solutions were more concentrated, the $n_2^{Kerr}$ values for these complexes would be much higher.

Moreover, for reference purposes, the value of the second hyperpolarizability of vildagliptin is compared with those corresponding to some small molecule nonlinear organic chromophores in Table 4 [35,36]. Even though these values have been measured in different solvents at 1.064 μm using the EFISH technique, they evidence the very high nonlinear optical response of vildagliptin when compared to other highly nonlinear materials of similar molecular complexity such as the stilbene derivative 4-dimethylamino-4′-nitrostilbene (DANS).

**Table 4. Comparison of the second hyperpolarizability of vildagliptin and some reference organic materials. The reference materials have been characterized at 1.064 μm using the EFISH.**

| | Empirical formula | Molecular weight (g/mol) | $\gamma$ (m$^5$/V$^2$) |
|---|---|---|---|
| *Vildagliptin* | *$C_{17}H_{25}N_3O_2$* | *303.40* | *$6.0 \times 10^{-46}$* |
| o-Nitroaniline | $C_6H_6N_2O_2$ | 138.12 | $3.4 \times 10^{-48}$ |
| p-Nitroaniline | $C_6H_6N_2O_2$ | 138.12 | $1.5 \times 10^{-47}$ |
| 4-Chlorostilbene | $C_{14}H_{11}Cl$ | 214.69 | $3.8 \times 10^{-49}$ |
| 4-Chloro-4'-dimethylaminostilbene | $C_{16}H_{16}ClN$ | 257.76 | $1.4 \times 10^{-47}$ |
| 4-Nitro-4'-aminostilbene | $C_{14}H_{12}N_2O_2$ | 240.09 | $1.4 \times 10^{-46}$ |
| DANS | $C_{16}H_{16}N_2O_2$ | 268.31 | $2.4 \times 10^{-46}$ |

With regard to the ytterbium(III) complexes, the $\gamma$ values are similar to those reported for transition metal tetrakis-(cumylphenoxy)phthalocyanines [4] and one order of magnitude lower than those attained by Sheng et *al*. for the larger double and triple-decker sandwich-

#228473 - $15.00 USD Received 25 Nov 2014; revised 15 Jan 2015; accepted 17 Jan 2015; published 6 Feb 2015

type mixed (phthalocyaninato)(porphyrinato) europium(III) complexes [5] and by Hou *et al.* for an octameric lanthanum(III) complex [9]. However, the incorporation of vildagliptin in ytterbium(III) complexes permits to obtain multifunctional materials that, with a higher molecular complexity, combine optical gain in the telecom windows with a very high second hyperpolarizability, of the order of magnitude of that of vildagliptin.

Computational analysis

Computational studies on the nonlinear optical properties of lanthanide complexes are extremely scarce [37]. The number of atoms forming the molecules can be very large and the reduced computer load associated to semi-empirical methods may result in a very interesting alternative to more accurate *ab-initio* calculations. Semi-empirical results tend to be qualitative and the agreement with experiments depends on the type of system that is analysed [4]. The comparison of semi-empirical quantum chemistry calculations with the experimental data permits us to assess the predictive power of this technique regarding the nonlinear optical properties of our complexes.

Figure 8 displays the average value over the tensor components of the second hyperpolarizability $\gamma_{abcd}(-\omega;\omega,-\omega,\omega)$ contributing to the intensity dependent refractive index in atomic units using the time-dependent Hartree-Fock method implemented in MOPAC [23]. The static values are shown in the first row of the table (see inset in Fig. 8). The remaining rows show the results evaluated at different wavelengths within the three telecommunication windows.

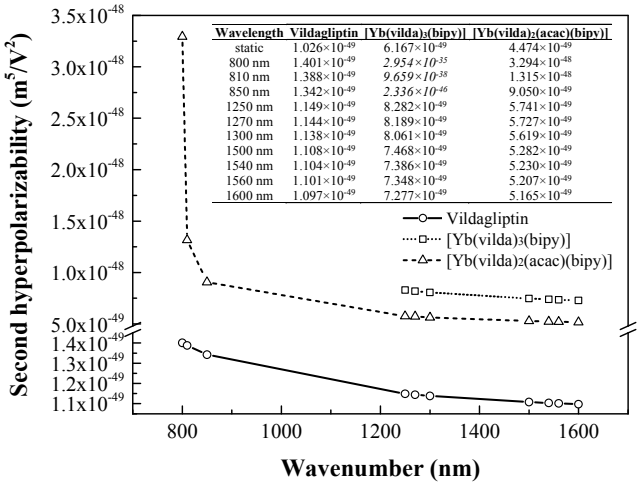


| Wavelength | Vildagliptin | [Yb(vilda)$_3$(bipy)] | [Yb(vilda)$_2$(acac)(bipy)] |
|---|---|---|---|
| static | $1.026\times10^{-49}$ | $6.167\times10^{-49}$ | $4.474\times10^{-49}$ |
| 800 nm | $1.401\times10^{-49}$ | *$2.954\times10^{-35}$* | $3.294\times10^{-48}$ |
| 810 nm | $1.388\times10^{-49}$ | *$9.659\times10^{-38}$* | $1.315\times10^{-48}$ |
| 850 nm | $1.342\times10^{-49}$ | *$2.336\times10^{-46}$* | $9.050\times10^{-49}$ |
| 1250 nm | $1.149\times10^{-49}$ | $8.282\times10^{-49}$ | $5.741\times10^{-49}$ |
| 1270 nm | $1.144\times10^{-49}$ | $8.189\times10^{-49}$ | $5.727\times10^{-49}$ |
| 1300 nm | $1.138\times10^{-49}$ | $8.061\times10^{-49}$ | $5.619\times10^{-49}$ |
| 1500 nm | $1.108\times10^{-49}$ | $7.468\times10^{-49}$ | $5.282\times10^{-49}$ |
| 1540 nm | $1.104\times10^{-49}$ | $7.386\times10^{-49}$ | $5.230\times10^{-49}$ |
| 1560 nm | $1.101\times10^{-49}$ | $7.348\times10^{-49}$ | $5.207\times10^{-49}$ |
| 1600 nm | $1.097\times10^{-49}$ | $7.277\times10^{-49}$ | $5.165\times10^{-49}$ |

Fig. 8. Second hyperpolarizabilities calculated with MOPAC2012 using the Sparkle/PM6 model.

Even though these are microscopic results corresponding to the response of a single isolated molecule, a high correlation with the macroscopic nonlinear refractive index for the average of the optical field over a domain enclosing a large number of molecules is expected [38]. The results for the two new complexes and pure vildagliptin show a very small dispersion in the nonlinear refractive index in the second and third optical communications windows. The computed nonlinear refractive index of all three species shows a steady spectral growth as we approach the visible part of the spectrum. This happens much more markedly in the case of [Yb(vilda)$_3$(bipy)], for which the values of the second hyperpolarizability in the first telecom window are too large to be accepted as realistic. The same type of exponential growth is found for [Yb(vilda)$_2$(acac)(bipy)] at shorter wavelengths, with a value of $3.358 \times 10^{-42}$ m$^5$/V$^2$ at 750 nm. The calculations for the nonlinear refractive index of vildagliptin are found to be stable at least up to 650 nm.

#228473 - $15.00 USD Received 25 Nov 2014; revised 15 Jan 2015; accepted 17 Jan 2015; published 6 Feb 2015

For all the wavelengths studied, and also in the static case, the two new complexes display an enhancement of the nonlinear refraction as compared to that of pure vildagliptin. Moreover, the predicted molecular hyperpolarizability term contributing to the nonlinear refractive index of [Yb(vilda)$_3$(bipy)] is larger than that of [Yb(vilda)$_2$(acac)(bipy)] in all the cases. This lack of consistency with the experimental results (which evince a larger $\gamma$ in [Yb(vilda)$_2$(acac)(bipy)]) can be ascribed to the limited accuracy of semi-empirical methods in the calculation of the nonlinear optical response of materials. Moreover, the values of the second hyperpolarizabilities of all the materials studied in this work are largely underestimated in the semiempirical calculations. Whereas this theoretical framework has a very good accuracy in the prediction of ground state geometries of lanthanide complexes [18], the predictive power for the third-order optical properties of vildagliptin and its derivatives seems to be seriously limited.

## 4. Conclusions

The nonlinear optical properties of vildagliptin have been investigated, together with the effect of the presence of two and three units coordinated to the same complex as ligands so as to determine their impact on the behavior of these novel materials. Very large second hyperpolarizabilities have been measured in all the materials studied. In the complex [Yb(vilda)$_3$(bipy)], the value of the nonlinear Kerr refractive index is slightly lower than that vildagliptin. Nevertheless, against the odds, the complex in which a vildagliptin unit had been substituted by a $\beta$-diketone (Hacac), [Yb(vilda)$_2$(acac)(bipy)], evinces a higher $\gamma$ value (23% higher than that vildagliptin). We consider that this could be attributed, more than to a favorable effect of acac, to a structural factor: the higher symmetry in the [Yb(vilda)$_2$(acac)(bipy)] molecule may have a beneficial effect.

## Acknowledgments

J.A. Novoa-López would like to thank University of Vigo for its financial support under "Axudas predoutorais: Áreas de especial dificultade" PhD scholarship program. Support by Xunta de Galicia under projects K133131H64102 and K044131H64502 is gratefully acknowledged by P. Chamorro-Posada, H. Michinel and P. Martín-Ramos are grateful to Junta de Castilla y León for providing funds under project VA300A12-1.

#228473 - $15.00 USD Received 25 Nov 2014; revised 15 Jan 2015; accepted 17 Jan 2015; published 6 Feb 2015